Electronic Supplementary Material (ESI) for Chemical Communications

Identifying the intermolecular hydrogen-bonding supramolecular synthons in an indomethacin-nicotinamide cocrystal by solid-state NMR

Keisuke Maruyoshi, Dinu Iuga, Oleg N. Antzutkin,
Amjad Alhalaweh, Sitaram P. Velaga, Steven P. Brown

S1. Preparation and Characterisation of the Indomethacin-Nicotinamide (IND-NIC) Cocrystal

S1.1 Preparation of IND-NIC Cocrystals

The IND-NIC cocrystal is congruently saturating in ethyl acetate and is thus prepared by the slurry method in this solvent.[1,2] A total of 3.578 g of IND and 1.221 g of NIC in a 1:1 molar ratio in 10 mL of ethyl acetate was taken in a flat bottom flask and stirred for 5 days at room temperature with the help of a magnetic stir bar on a stir plate. Solids were filtered, dried and analyzed by differential scanning calorimetry and powder X-ray diffractometry.

S1.2 Differential scanning calorimetry (DSC)

Thermal analyses of the samples were performed on a DSC Q1000 (TA instrument) which was calibrated for temperature and enthalpy using an indium standard. The samples (1-3 mg) were crimped in non-hermetic aluminium pans and scanned at a heating rate of 10 °C/min under a continuously purged dry nitrogen atmosphere (flow rate 50 mL/min). The instrument was equipped with a refrigerated cooling system.

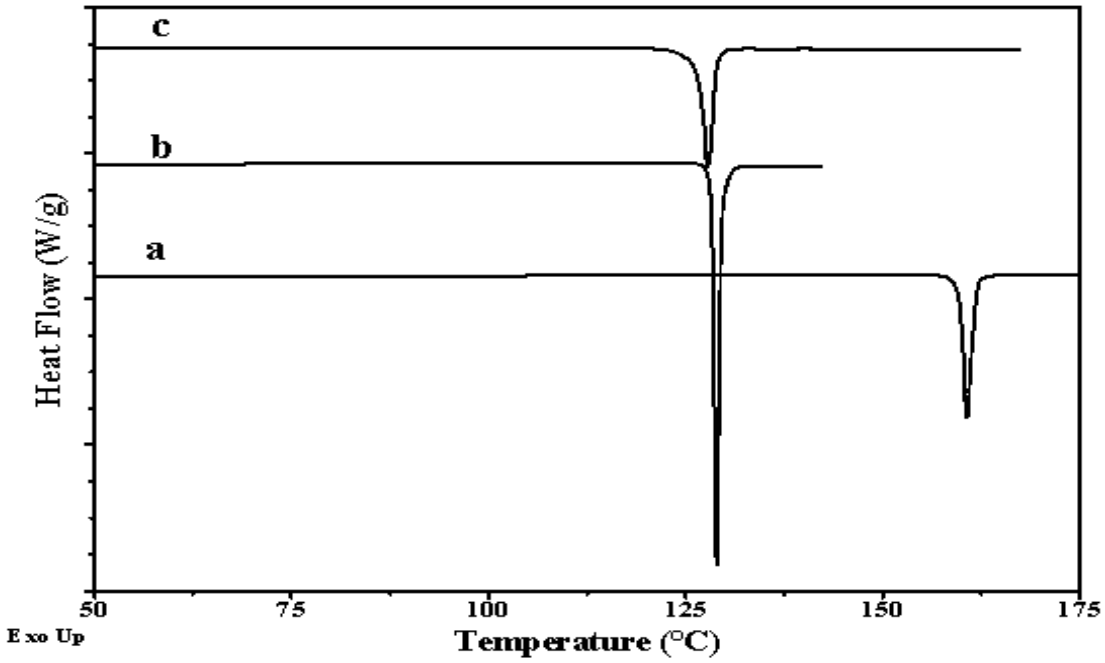

Fig. S1. DSC heating curves of a) IND (γ-form) as received, b) NIC as received and c) IND-NIC cocrystal.

S1.3 Powder X-ray diffraction (PXRD)

PXRD patterns were recorded on a Siemens D5000 powder diffractometer with CuKα radiation (1.54056 Å). The tube voltage and amperage were set at 40 kV and 40 mA, respectively. The divergence slit and anti-scattering slit settings were variable for the illumination of the 20 mm sample size. Each sample was scanned over a range of 2θ between 5° and 40° with a step size of 0.02° or 0.05° and a time per step of 1 second. The instrument was previously calibrated using a silicon standard.

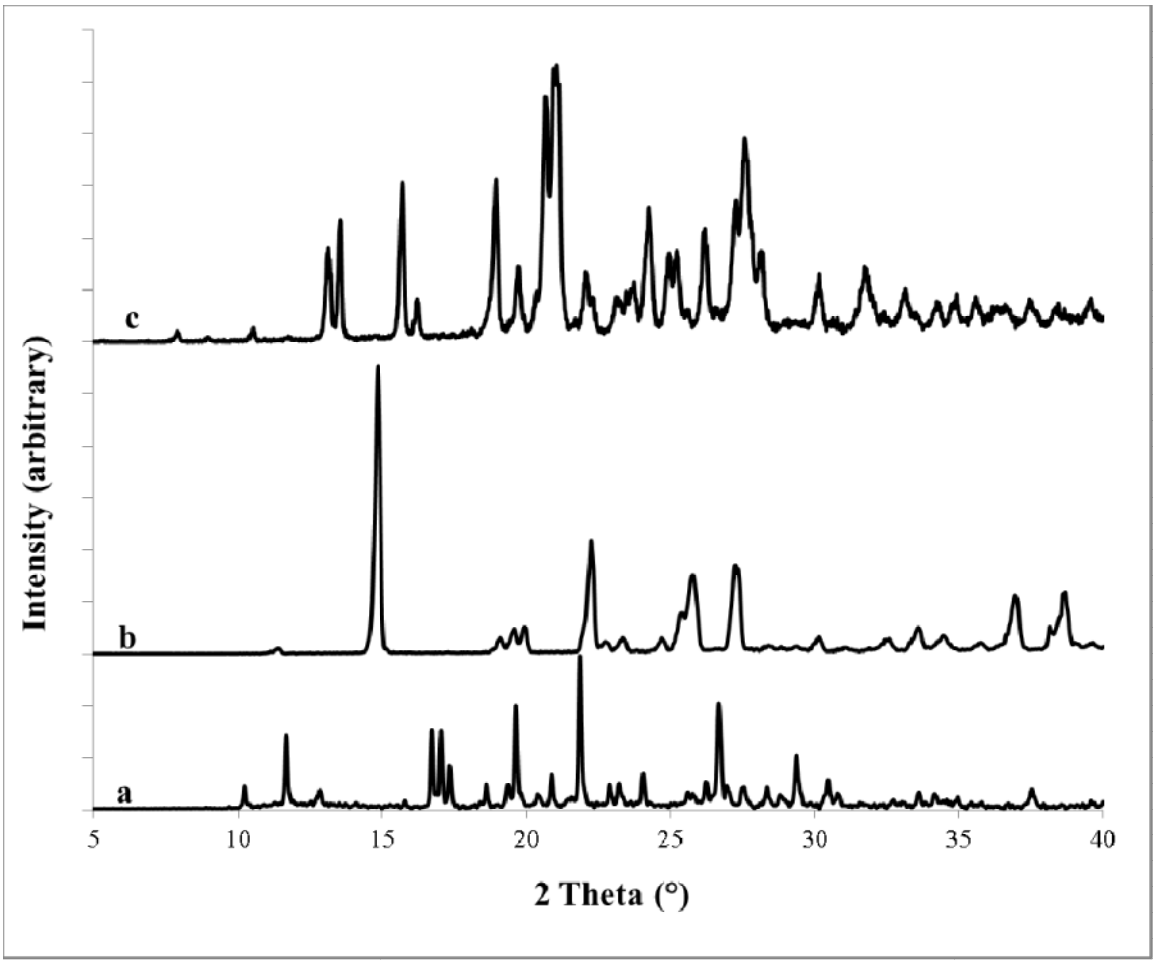

Fig. S2. PXRD patterns of a) IND (γ-form) as received, b) NIC as received (intensity reduced five times for clarity) and c) IND-NIC cocrystal.

S2. Full Experimental Solid-State NMR Details

Pulse sequences and coherence transfer pathway diagrams for the (a) ^{1}H DQ MAS[3] using BABA (back-to-back) recoupling[4,5], (b) 2D ^{14}N-^{1}H HMQC[6] and (c) ^{1}H (SQ-DUMBO) – ^{13}C SQ refocused INEPT (2D INEPT HSQC)[7] experiments are shown in Fig. 7 of Ref.[8], Fig. 3a of Ref.[6] and Fig. 5 of Ref.[7], respectively.

2D ^{1}H DQ and ^{1}H–^{13}C experiments were performed on a Bruker Avance III spectrometer operating at Larmor frequencies of 500.1 MHz for ^{1}H and 125.8 MHz for ^{13}C (B_0 = 11.7 T) using a Bruker 4.0 mm triple-resonance probe, operating in double-resonance mode, at 12.5 kHz MAS for the 2D INEPT HSQC experiment or a Bruker 2.5 mm triple-resonance, operating in double-resonance mode, at 30 kHz MAS for the 2D ^{1}H DQ MAS experiment. In all experiments, the ^{1}H and ^{13}C 90^{o} pulse lengths were 2.5 μs and 5.0 μs, respectively.

For the 2D ^{1}H DQ MAS experiment, 16 transients were co-added for each of 88 t_1 FIDs (with a rotor-synchronised t_1 increment of 33.3 μs using the States-TPPI method to achieve sign discrimination in F_1), with a recycle delay of 3 s. A 16-step phase cycle was used to select $\Delta p = \pm 2$ on the DQ excitation block and $\Delta p = -1$ on the final 90^{o} pulse, where p is the coherence order.

For the 2D ^{1}H–^{13}C INEPT HSQC experiment, eDUMBO-1$_{22}$ homonuclear decoupling,[9,10] at a ^{1}H nutation frequency of 100 kHz, was employed during the τ and τ′ free-evolution periods in the refocused INEPT element of the ^{1}H-^{13}C correlation experiments: τ = τ’ equalled 1.28 ms. The 32 μs eDUMBO-1$_{22}$ cycle was divided into 320 steps of 100 ns. Pulse sequences employing ^{1}H homonuclear decoupling use pre-pulses to take into account the tilting of the effective field away from the x, y plane of the rotation frame:[11] A pre-pulse duration of 0.7 μs was used. For acquisition under ^{1}H homonuclear decoupling, a short detection window was inserted after every eDUMBO-1$_{22}$ cycle in t_2 in order to acquire a complex point. The scaling factor was determined experimentally (by using the ^{1}H chemical shifts of the resolved resonances in a ^{1}H 30 kHz MAS spectrum) as 1.77. During the acquisition of the ^{13}C FID in t_2, ^{1}H SPINAL-64 heteronuclear decoupling[12] with a pulse length of 4.6 μs was applied at a ^{1}H nutation frequency of 100 kHz. 128 transients were co-added for each of 112 t_1 FIDs (with a t_1 increment of 64 μs, using the States method to achieve sign discrimination in F_1), with a recycle delay of 3 s. A 16-step phase cycle was used as described in Ref.[7].

2D ^{14}N-^{1}H HMQC experiments were recorded using a Bruker Avance III

spectrometer operating at Larmor frequencies of 850.2 MHz for ^{1}H and 61.4 MHz for ^{14}N (B_0 = 20.0 T) using a Bruker 1.3 mm triple-resonance probe, operating in double-resonance mode, at 60 kHz MAS. ^{1}H 90^{o} pulses of duration 1.9 μs were used, while ^{14}N pulses of duration 8.0 μs at a nutation frequency of 125 kHz were used. Rotary resonance recoupling (R^3)[13] was applied at the n = 2 condition with a phase inversion (0°, 180°)[14] on each pair of rotor-synchronised pulses which are each of duration 16.7 μs. For a rotor-synchronised t_1 increment of 16.7 μs using the States method to achieve sign discrimination in F_1, 68 transients were co-added for each of 48 t_1 FIDs (recoupling time equal to 130 μs) or 42 t_1 FIDs (recoupling time equal to 670 μs). A recycle delay of 10 s was used. A 4-step nested phase cycle was used to select changes in coherence order $\Delta p = \pm 1$ (on the first ^{1}H pulse, 2 steps) and $\Delta p = \pm 1$ (on the last ^{14}N pulse, 2 steps).

^{13}C and ^{1}H chemical shifts are referenced with respect to neat TMS using adamantane as a secondary reference (38.5 ppm for the higher-ppm ^{13}C resonance[15] and 1.85 ppm for the ^{1}H resonance[16] – note the small correction to the ^{1}H referencing as compared to previous papers). Experimental ^{13}C and ^{1}H chemical shifts are stated to an accuracy of ±0.1 or 0.2 ppm, respectively. ^{14}N shifts were referenced to a saturated NH_4Cl aqueous solution at –352.9 ppm, corresponding to a primary reference of CH_3NO_2 at 0 ppm. To convert to the corresponding ^{15}N chemical shift scale frequently used in protein NMR, where the reference is liquid ammonia at –50°C, it is necessary to add 379.5 to the given values.[17]

S3. ^{1}H and ^{13}C Chemical Shifts

Table S1. ^{1}H & ^{13}C chemical shifts for the indomethacin-nicotinamide cocrystal

Site	$\delta(^{1}H)$ (ppm)	$\delta(^{13}C)$ (ppm)
	Indomethacin	
1		133.5
2		112.6
3		130.8
4	6.8	103.6
5		156.3
6	5.5	106.5
7	7.3	113.1
8		128.8
9 (a&b)	3.4	30.4
10		176.0
11	2.9	55.2
12	0.9	12.9
13		167.7
14		130.8
15	6.4	130.8
16	6.0	127.9
17		134.2
18	6.0	128.8
19	6.4	130.8
OH	16.3	
	Nicotinamide	
1	9.8	147.0
2		130.8
3	7.7	139.5
4	8.3	125.8
5	9.8	149.7
6		167.7
NH_2 a	9.0	
NH_2 b	7.3	

S4. Complete ^{1}H DQ MAS Spectrum

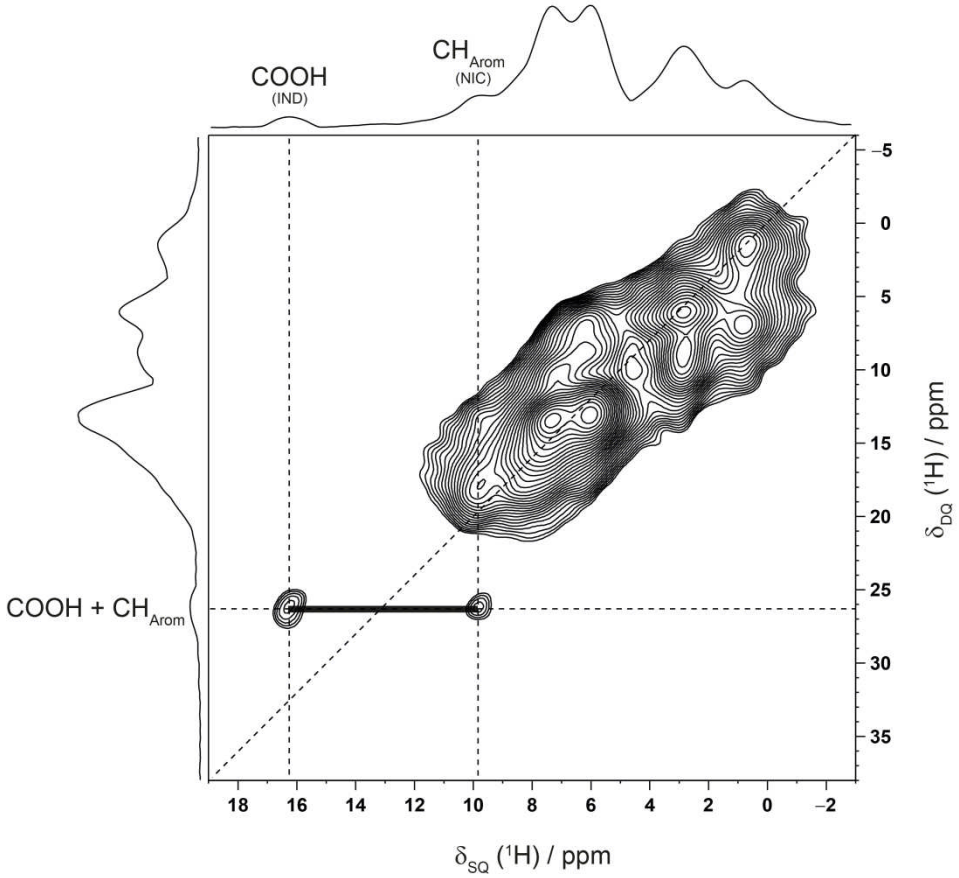

Fig. S3. Complete ^{1}H DQ MAS spectrum, corresponding to the zoomed region presented in Fig. 1a of the main text.

S5. Complete ^{14}N-^{1}H Spectrum

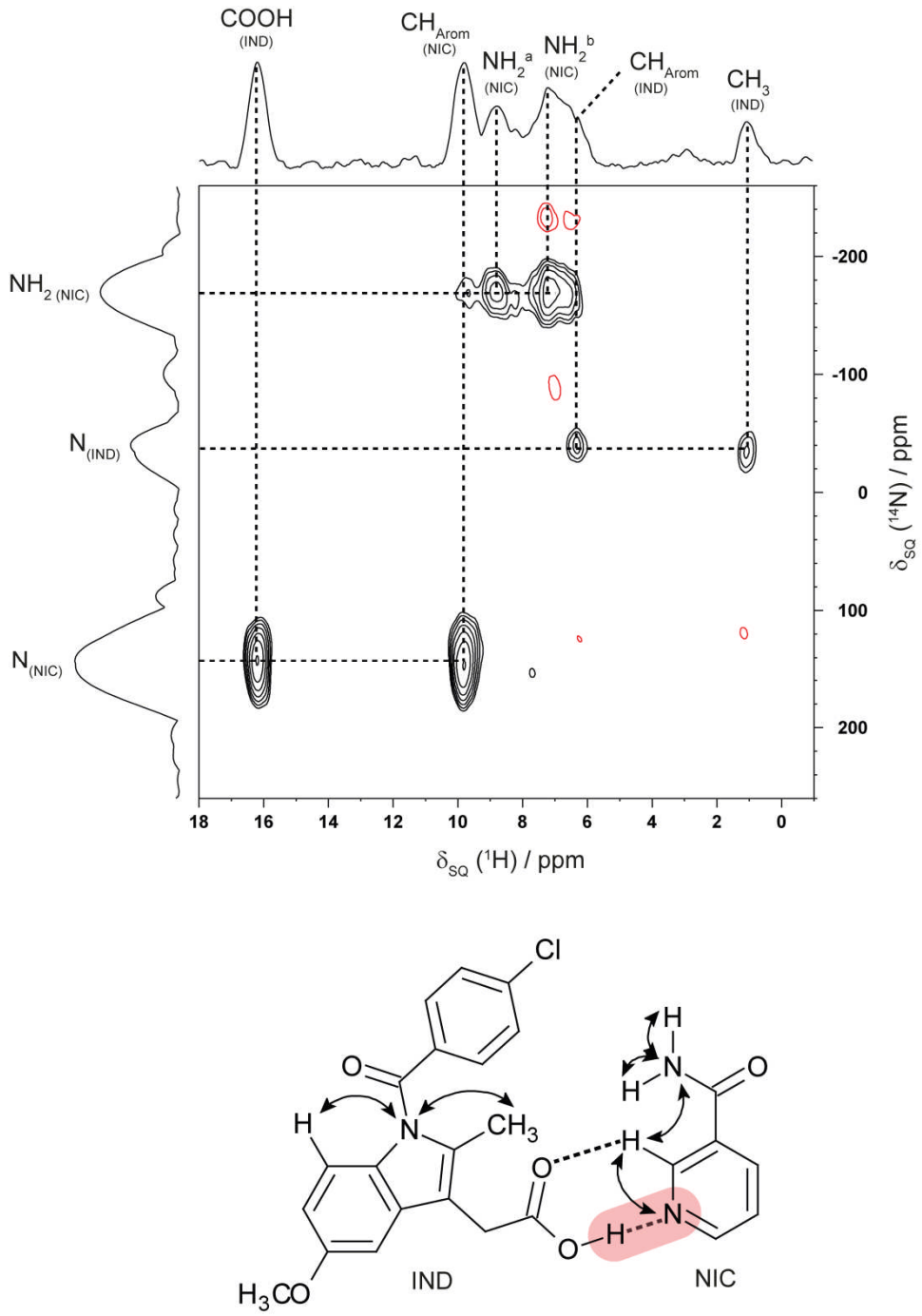

Fig. S4. Complete ^{14}N-^{1}H spectrum, corresponding to the zoomed region presented in Fig. 1c of the main text.

S6. Complete ^{1}H-^{13}C Spectrum

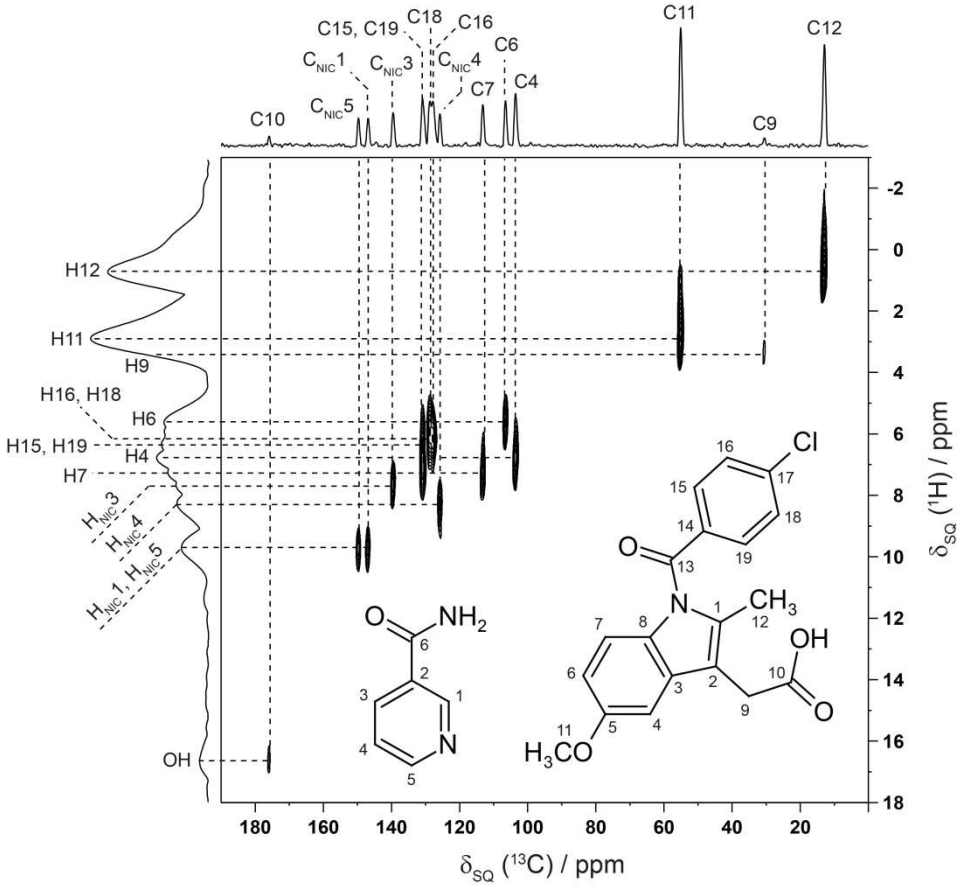

Fig. S5. Complete ^{1}H-^{13}C spectrum, corresponding to the zoomed region presented in Fig. 1d of the main text.

References

1 A. Alhalaweh and S. P. Velaga, *Cryst. Growth Des.*, 2010, **10**, 3302.
2 A. Alhalaweh, A. Sokolowski, N. Rodriguez-Hornedo, and S. P. Velaga, *Cryst. Growth Des.*, 2011, **11**, 3923.
3 S. P. Brown, *Prog. Nucl. Magn. Reson. Spectrosc.*, 2007, **50**, 199.
4 W. Sommer, J. Gottwald, D. E. Demco, and H. W. Spiess, *J. Magn. Reson. Ser. A*, 1995, **113**, 131.
5 I. Schnell, A. Lupulescu, S. Hafner, D. E. Demco, and H. W. Spiess, *J. Magn. Reson.*, 1998, **133**, 61.
6 Z. H. Gan, J. P. Amoureux, and J. Trebosc, *Chem. Phys. Lett.*, 2007, **435**, 163.
7 B. Elena, A. Lesage, S. Steuernagel, A. Bockmann, and L. Emsley, *J. Am. Chem. Soc.*, 2005, **127**, 17296.
8 S. P. Brown and H. W. Spiess, *Chem. Rev.*, 2001, **101**, 4125.
9 D. Sakellariou, A. Lesage, P. Hodgkinson, and L. Emsley, *Chem. Phys. Lett.*, 2000, **319**, 253.
10 B. Elena, G. de Paepe, and L. Emsley, *Chem. Phys. Lett.*, 2004, **398**, 532.
11 A. Lesage, D. Sakellariou, S. Hediger, B. Elena, P. Charmont, S. Steuernagel, and L. Emsley, *J. Magn. Reson.*, 2003, **163**, 105.
12 A. Khitrin and B. M. Fung, *J. Chem. Phys.*, 2000, **112**, 2392.
13 T. G. Oas, R. G. Griffin, and M. H. Levitt, *J. Chem. Phys.*, 1988, **89**, 692.
14 P. R. Costa, J. D. Gross, M. Hong, and R. G. Griffin, *Chem. Phys. Lett.*, 1997, **280**, 95.
15 C. R. Morcombe and K. W. Zilm, *J. Magn. Reson.*, 2003, **162**, 479.
16 S. Hayashi and K. Hayamizu, *Bull. Chem. Soc. Jpn.*, 1991, **64**, 685.
17 G. E. Martin and C. E. Hadden, *J. Nat. Prod.*, 2000, **63**, 543.